Journal of Power Sources 206 (2012) 197–203

Contents lists available at SciVerse ScienceDirect

Journal of Power Sources

journal homepage: www.elsevier.com/locate/jpowsour

Optimization studies of a polymer electrolyte membrane fuel cell with multiple catalyst layers

Modekurti Srinivasarao[a], Debangsu Bhattacharyya[b,*], Raghunathan Rengaswamy[c]

[a] Department of Chemical Engineering, Indian Institute of Technology Madras, Chennai 600 036, India
[b] Department of Chemical Engineering, West Virginia University, Morgantown, WV 26506, USA
[c] Department of Chemical Engineering, Texas Tech University, Lubbock, TX 79409, USA

ARTICLE INFO

Article history:
Received 31 October 2011
Received in revised form 23 January 2012
Accepted 23 January 2012
Available online 1 February 2012

Keywords:
PEMFC
Optimization
Multiple catalyst layers
Platinum loading

ABSTRACT

To make the polymer electrolyte membrane fuel cells (PEMFC) commercially viable, further reduction in cost and improvement in performance are required. In this work, an innovative design of a PEMFC with multiple catalyst layers (CLs) is considered and the design variables, weight fraction of platinum on carbon (f_{pt}), platinum loading (m_{pt}), ionomer loading ($f_{ionomer}$) and thickness of all the CLs, are optimized for cost reduction and performance enhancement. In the first optimization study, the cell performance is maximized. The maximum current density of an optimized PEMFC with four CLs shows a significant improvement over the base case design at all operating voltages. In another optimization study, the platinum loading of the PEMFC with multiple CLs is minimized. With an increase in the number of catalyst layers, the platinum required to achieve the base case design current density is reduced. Using four CLs, a reduction of 17% (at 0.15 A cm^{-2}) to 60% (at 0.7 A cm^{-2}) in platinum loading is achieved in comparison to the base case design. In addition, the maximum power density of the PEMFC with multiple CLs is found to be superior to that of an optimized PEMFC with a single CL at all voltages.

1. Introduction

The cathode catalyst layer (CL) is one of the most important layers of a polymer electrolyte membrane fuel cell (PEMFC). Some of the issues that have hindered commercialization of the PEMFCs are: (i) under-utilization of the electro-catalyst (ii) lower performance due to mass transfer losses, ionic and ohmic losses, and inadequate removal of liquid water from the reaction sites. To mitigate these problems, we investigated an innovative design of a PEMFC with multiple catalyst layers in one of our previous papers [1]. There are few other experimental and numerical studies that have also highlighted the advantages of multiple catalyst layers over the conventional single layer [2–4]. The motivation for using multiple catalyst layers is to vary the design parameters of a CL spatially according to the operational requirement of a PEMFC. The CL adjacent to the diffusion medium should be of higher porosity than the other CLs as the concentration of oxygen decreases in a CL from the diffusion medium-CL interface towards the polymer membrane. The CL adjacent to the polymer membrane should contain more ionomer than the other CLs. Furthermore, liquid water should be removed without causing significant mass transport and/or ohmic losses. Because of the difficulty in manufacturing such a continuously graded CL, a combination of layers can be synthesized where each layer is manufactured with different design parameters. Our previous paper showed the performance of the PEMFC with multiple CLs is superior to the PEMFCs with a single CL [1]. Motivated by these results we have performed optimization studies of a PEMFC with multiple CLs to further improve its performance and reduce its cost. The typical design parameters of the CL are: weight fraction of platinum on carbon (f_{pt}), platinum loading (m_{pt}) and ionomer loading ($f_{ionomer}$). For optimizing these design parameters, a detailed steady state model of a PEMFC cathode with multiple layers is required. In this work, we have considered our previously developed model with few modifications. The basic PEMFC configuration remains similar to before. The model considers liquid water in all the layers. The catalyst layer microstructure is modeled as a network of spherical agglomerates. This characterization is based on a previous study [5] that compared macro-homogenous and spherical agglomerate characterizations and observed that spherical agglomerate characterization is a better representation of the CL. For improved water management, a thin micro-porous layer is considered between the gas diffusion layer (GDL) and the first catalyst layer.

A few papers are available in the open literature on the cathode CL optimization. Song et al. [6] have obtained optimal distributions

Abbreviations: PEMFC, polymer electrolyte membrane fuel cell; GC, gas channel; GDL, gas diffusion layer; MPL, microporous layer; CL, catalyst layer; MEM, membrane; MEA, membrane electrode assembly; ORR, oxygen reduction reaction.

* Corresponding author. Tel.: +1 3042939335; fax: +1 3042934139.
E-mail address: Debangsu.Bhattacharyya@mail.wvu.edu (D. Bhattacharyya).

0378-7753/$ – see front matter © 2012 Elsevier B.V. All rights reserved.
doi:10.1016/j.jpowsour.2012.01.135

Nomenclature

C_i^k	concentration of species i in region k (mol m^{-3})
$C_{i,o}$	Inlet concentrations of i (mol m^{-3})
$C_{O_2}\|_{ns}$	concentration of dissolved oxygen at the interface of ionomer and agglomerate (mol m^{-3})
C_W^{mem}	concentration of liquid water in the membrane (mol m^{-3})
$D_i^{eff,k}$	effective diffusivity of the species i in region k (m^2 s^{-1})
$D_{O_2}^{mem}$	diffusivity of oxygen in ionomer (m^2 s^{-1})
D_W^{mem}	diffusivity of liquid water in the membrane (m^2 s^{-1})
$f_{ionomer}$	weight fraction of ionomer in the catalyst layer
f_{pt}	weight fraction of platinum on carbon
F	Faraday's constant (C g^{-1} equiv.$^{-1}$)
i_{base}	current density for base case design conditions (A m^{-2} Pt^{-1})
i_{cell}	cell current density (A m^{-2} Pt^{-1})
i_{opt}	current density for optimized design (A m^{-2} Pt^{-1})
I_w	interfacial transfer of water between liquid and vapor (mol m^{-3} s^{-1})
J_i^k	local flux due to diffusion of species i in region k (mol m^{-2} s^{-1})
k_c	condensation constant (s^{-1})
k_v	evaporation constant (atm^{-1} s^{-1})
m_{Pt}	platinum loading inside the catalyst layer (kg Pt m^{-2} CL^{-1})
M_W	molecular weight of water (g mol^{-1})
n	number of electrons taking part in the oxygen reduction reaction
$N_{W,k}$	flux of liquid water in region k (mol m^{-2} s^{-1})
P_c	capillary pressure (atm)
p_w	partial pressure of water vapor (atm)
p_w^{sat}	saturation pressure of water vapor (atm)
q	switching function
r_{agg}	agglomerate radius (m)
R	universal gas constant (J mol^{-1} K^{-1})
R_{O_2}	rate of oxygen reduction reaction per unit volume of the catalyst layer (mol m^{-3} s^{-1})
s_k	liquid water saturation level in region k
T_{cell}	cell temperature (K)
t_{CL}	thickness of the catalyst layer (m)
V_{Cell}	cell voltage (V)
y_w	mole fraction of water in the gas phase

Greek letters

α_a	vapor activity in the gas phase in the anode catalyst layer
α_c	vapor activity in the gas phase in the cathode catalyst layer
ε_k	void fraction inside region k
$\varepsilon_{ionomer}$	fraction of volume occupied by the ionomer inside the catalyst layer
ξ	effectiveness factor
$\kappa^{eff,c}$	effective proton conductivity in the catalyst layer (mho m^{-1})
$\kappa^{eff,mem}$	effective proton conductivity in the membrane (mho m^{-1})
κ_{ele}^k	electric conductivity in region k (S m^{-1})
$\kappa_{ele}^{eff,k}$	effective electric conductivity in region k (S m^{-1})
ρ_c	density of carbon (kg m^{-3})
$\rho_{ionomer}$	density of ionomer (kg m^{-3})
ρ_{Pt}	density of platinum (kg m^{-3})
ρ_w	density of water (kg m^{-3})
ψ	Thiele modulus

Subscripts

i	index for the species: O_2, N_2, H_2O
k	index for the region: diffusion layer, micro-porous layer, catalyst layer

of platinum and Nafion for the maximization of current density at a given voltage. The authors concluded that the optimal distribution of Nafion content is a linearly increasing function and the optimal distribution of platinum is a convex increasing function across the thickness of the catalyst layer. Lin et al. [7] optimized the channel to width ratio, porosity of the GDL, and porosity of the catalyst layer. Secanell et al. [8] performed multivariable optimization studies of the PEMFC cathode. The authors considered platinum loading, volume fraction of the ionomer in the agglomerate, fraction of the platinum on carbon, and porosity of the GDL as decision variables. The authors suggested that the performance at medium and high current densities can be improved by increasing the ionomer content and reducing the carbon and platinum loadings. The authors did not consider the liquid water effect on the cell performance. The liquid water generated in the ORR reaction plays a major role especially in the mass transfer limiting regions. Later Jain et al. [9] reformulated the agglomerate model of Secanell et al. [8] into a condensed form for minimization of the platinum loading at various current densities. They obtained optimum platinum distribution along the CL width by dividing the CL into various zones.

Our group recently published a multivariable optimization study of a PEMFC cathode considering the effect of liquid water [10]. In the current work, multivariable optimization studies of a PEMFC with multiple CLs are performed. Two objective functions are considered here. In the first study, the objective is to maximize the cell current density for a given voltage. The second study focuses on minimization of the platinum loading for a given current density. The design parameters of all the catalyst layers are the decision variables for both the optimization studies.

2. Model description

Because of some modifications to the previously developed model [1] and to ensure completeness, the model used in the optimization studies is briefly described here. The schematic of the model domain considered in this study is shown in Fig. 1. The cathode flow field consists of parallel channels. The reactants fed to the channels diffuse to the CL through the gas diffusion layer (GDL) and micro-porous layer (MPL). The two-dimensional two-phase model with four CLs considers transport of the reactant gases, O_2, N_2, and H_2O (v), in the GDL, MPL, and CLs. In addition, liquid water transport in the membrane (considering both electro-osmotic drag and back diffusion), CLs, MPL, and GDL is considered. Furthermore, protons transport in the membrane and CLs, and electrons transport in the GDL, MPL, and CLs are modeled. Electrochemical oxygen reduction reaction (ORR) is considered in all the CLs. The model assumptions are: (i) isothermal, isobaric, and steady-state operation; (ii) water generated due to ORR is in liquid form; (iii) physical properties of ionomer in all the CLs and in the membrane is same; (iv) negligible contact resistance between the cathode layers. The model equations and boundary conditions are shown in Tables 1 and 2, respectively. The system of equations is solved using a combination of MAPLE® and MATLAB®. The partial differential equations (PDEs) along with the boundary conditions are written in MAPLE®. The PDEs are discretized

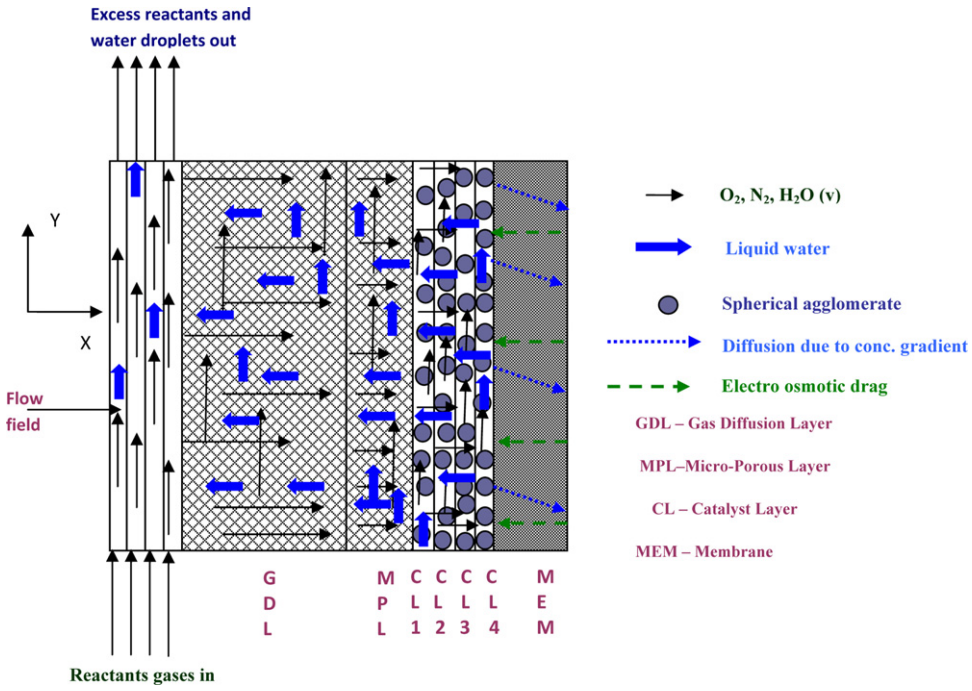

Fig. 1. Schematic of the model domain.

Table 1
Conservation equations (C = concentration, J = gas flux, N = liquid flux).

Variables	Gas channel	Diffusion layer (DL)	Micro porous layer (MPL)	Catalyst layers (CLs)	Polymer membrane
C_{O_2}	$-\frac{\partial}{\partial y}(C_{O_2}u) - \nabla \cdot J_{O_2} = 0$	$-\nabla \cdot (-D_{O_2}^{eff,d}\nabla C_{O_2}) = 0$	$-\nabla \cdot (-D_{O_2}^{eff,m}\nabla C_{O_2}) = 0$	$-\nabla \cdot (-D_{O_2}^{eff,c}\nabla C_{O_2}) - R_{O_2} = 0$	–
C_{N_2}	$-\frac{\partial}{\partial y}(C_{N_2}u) - \nabla \cdot J_{N_2} = 0$	$-\nabla \cdot (-D_{N_2}^{eff,d}\nabla C_{N_2}) = 0$	$-\nabla \cdot (-D_{N_2}^{eff,m}\nabla C_{N_2}) = 0$	$-\nabla \cdot (-D_{N_2}^{eff,c}\nabla C_{N_2}) = 0$	–
C_{H_2O}	$-\frac{\partial}{\partial y}(C_{H_2O}u) - \nabla \cdot J_{H_2O} - I_W = 0$	$-\nabla \cdot (-D_{H_2O}^{eff,d}\nabla C_{H_2O}) - I_W = 0$	$-\nabla \cdot (-D_{H_2O}^{eff,m}\nabla C_{H_2O}) - I_W = 0$	$-\nabla \cdot (-D_{H_2O}^{eff,c}\nabla C_{H_2O}) - I_W = 0$	–
s	$-\frac{\rho_W}{M_W}\frac{\partial}{\partial y}(su) - \nabla \cdot N_{W,d} + I_W = 0$	$-\nabla \cdot N_{W,d} + I_W = 0$	$-\nabla \cdot N_{W,m} + I_W = 0$	$-\nabla \cdot N_{W,c} + I_W + 2R_{O_2} = 0$	$-\nabla \cdot N_{W,mem} = 0$
ϕ_r	–	–	–	$\kappa^{eff,c}\nabla^2\varphi_r + nFR_{O_2} = 0$	$-\kappa^{eff,mem}\nabla^2\varphi_r = 0$
ϕ_s	–	$-\kappa_{ele}^{eff,d}\nabla^2\phi_s = 0$	$-\kappa_{ele}^{eff,m}\nabla^2\phi_s = 0$	$\kappa_{ele}^{eff,c}\nabla^2\phi_s - nFR_{O_2} = 0$	

Where $I_w = k_c(\varepsilon_k(1-s)/RT_{cell})y_w(p_w - p_w^{sat})q + k_v(\varepsilon_k s\rho_w/M_w)(p_w - p_w^{sat})(1-q)$ (interfacial transfer of water between liquid and vapor phases) and $R_{O_2} = -\xi k_{rxn}C_{O_2}|_{ns}$ (rate of oxygen consumption).

Table 2
Boundary conditions in thickness direction.

Variables	C_{O_2}	C_{N_2}	C_{H_2O}	s	ϕ_r	ϕ_s
Entrance	$C_{O_2} = C_{O_2,o}$	$C_{N_2} = C_{N_2,o}$	$C_{H_2O} = C_{H_2O,o}$	0	–	–
GC/DL	$C_{O_2}^{GC} = C_{O_2}^{DL}$	$C_{N_2}^{GC} = C_{N_2}^{DL}$	$C_{H_2O}^{GC} = C_{H_2O}^{DL}$	$s^{GC} = s^{DL}$	–	$\phi_s^{DL} = V_{cell}$
DL/MPL	$C_{O_2}^{DL} = C_{O_2}^{MPL}$	$C_{N_2}^{DL} = C_{N_2}^{MPL}$	$C_{H_2O}^{DL} = C_{H_2O}^{MPL}$	$p_c^{DL} = p_c^{MPL}$		$\kappa_{ele}^{eff,d}\nabla\phi_{s\|DL} = \kappa_{ele}^{eff,m}\nabla\phi_{s\|MPL}$
	$J_{O_2}^{DL} = J_{O_2}^{MPL}$	$J_{N_2}^{DL} = J_{N_2}^{MPL}$	$J_{H_2O}^{DL} = J_{H_2O}^{MPL}$	$N_W^{DL} = N_W^{MPL}$	–	$\phi_s^{DL} = \phi_s^{MPL}$
MPL/CL1	$C_{O_2}^{MPL} = C_{O_2}^{CL1}$	$C_{N_2}^{MPL} = C_{N_2}^{CL1}$	$C_{H_2O}^{MPL} = C_{H_2O}^{CL1}$	$p_c^{MPL} = p_c^{CL1}$	$\nabla\phi_r = 0$	$\kappa_{ele}^{eff,m}\nabla\phi_{s\|MPL} = \kappa_{ele}^{eff,CL1}\nabla\phi_{s\|CL1}$
	$J_{O_2}^{MPL} = J_{O_2}^{CL1}$	$J_{N_2}^{MPL} = J_{N_2}^{CL1}$	$J_{H_2O}^{MPL} = J_{H_2O}^{CL1}$	$N_W^{MPL} = N_W^{CL1}$		$\phi_s^{MPL} = \phi_s^{CL1}$
CL1/CL2	$C_{O_2}^{CL1} = C_{O_2}^{CL2}$	$C_{N_2}^{CL1} = C_{N_2}^{CL2}$	$C_{H_2O}^{CL1} = C_{H_2O}^{CL2}$	$p_c^{CL1} = p_c^{CL2}$	$\phi_{r\|CL1} = \phi_{r\|CL2}$	$\kappa_{ele}^{eff,CL1}\nabla\phi_{s\|CL1} = \kappa_{ele}^{eff,CL2}\nabla\phi_{s\|CL2}$
	$J_{O_2}^{CL1} = J_{O_2}^{CL2}$	$J_{N_2}^{CL1} = J_{N_2}^{CL2}$	$J_{H_2O}^{CL1} = J_{H_2O}^{CL2}$	$N_W^{CL1} = N_W^{CL2}$	$\kappa^{eff,CL1}\nabla\phi_{r\|CL1} = \kappa^{eff,CL2}\nabla\phi_{r\|CL2}$	$\phi_s^{CL1} = \phi_s^{CL2}$
CL2/CL3	$C_{O_2}^{CL2} = C_{O_2}^{CL3}$	$C_{N_2}^{CL2} = C_{N_2}^{CL3}$	$C_{H_2O}^{CL2} = C_{H_2O}^{CL3}$	$p_c^{CL2} = p_c^{CL3}$	$\phi_{r\|CL2} = \phi_{r\|CL3}$	$\kappa_{ele}^{eff,CL2}\nabla\phi_{s\|CL2} = \kappa_{ele}^{eff,CL3}\nabla\phi_{s\|CL3}$
	$J_{O_2}^{CL2} = J_{O_2}^{CL3}$	$J_{N_2}^{CL2} = J_{N_2}^{CL3}$	$J_{H_2O}^{CL2} = J_{H_2O}^{CL3}$	$N_W^{CL2} = N_W^{CL3}$	$\kappa^{eff,CL2}\nabla\phi_{r\|CL2} = \kappa^{eff,CL3}\nabla\phi_{r\|CL3}$	$\phi_s^{CL2} = \phi_s^{CL3}$
CL3/CL4	$C_{O_2}^{CL3} = C_{O_2}^{CL4}$	$C_{N_2}^{CL3} = C_{N_2}^{CL4}$	$C_{H_2O}^{CL3} = C_{H_2O}^{CL4}$	$p_c^{CL3} = p_c^{CL4}$	$\phi_{r\|CL3} = \phi_{r\|CL4}$	$\kappa_{ele}^{eff,CL3}\nabla\phi_{s\|CL3} = \kappa_{ele}^{eff,CL4}\nabla\phi_{s\|CL4}$
	$J_{O_2}^{CL3} = J_{O_2}^{CL4}$	$J_{N_2}^{CL3} = J_{N_2}^{CL4}$	$J_{H_2O}^{CL3} = J_{H_2O}^{CL4}$	$N_W^{CL3} = N_W^{CL4}$	$\kappa^{eff,CL3}\nabla\phi_{r\|CL3} = \kappa^{eff,CL4}\nabla\phi_{r\|CL4}$	$\phi_s^{CL3} = \phi_s^{CL4}$
CL4/MEM	$\nabla C_{O_2}^{CL4} = 0$	$\nabla C_{N_2}^{CL4} = 0$	$\nabla C_{H_2O}^{CL4} = 0$	$C_W^{MEM} = C_W^{CL,EQ}(\alpha)$	$\phi_{r\|CL4} = \phi_{r\|MEM}$	$\nabla\phi_s^{CL4} = 0$
				$N_W^{CL4} = N_W^{MEM}$	$\kappa^{eff,CL4}\nabla\phi_{r\|CL4} = \kappa^{eff,mem}\nabla\phi_{r\|MEM}$	
MEM/ANODECL				$C_W^{MEM} = C_W^{CL,EQ}(\alpha^{anode})$	$\phi_r = 0$	

Table 3
Base case design decision variables.

Decision variable	Base case design
m_{pt} (mg cm^{-2})	0.4
f_{pt}	0.2
$f_{ionomer}$	0.34
t_{CL} (μm)	20

Table 4
Range of design parameters for optimization.

Decision variable (i = 1–4)	Lower bound	Upper bound
$m_{pt,i}$ (mg cm^{-2})	0.0125	0.1 and 0.25
$f_{pt,i}$	0.05	0.95
$f_{ionomer,i}$	0.05	0.95
$t_{CL,i}$ (μm)	2.5	5

in MAPLE® using forward difference technique. Analytical Jacobians are generated and then the system of equations along with the analytical Jacobians is exported to MATLAB®. The optimization is performed in MATLAB® using the function "fmincon" available in the MATLAB's optimization tool box. The constrained nonlinear optimization has been carried out by a feasible path approach in which the PEMFC model equations are converged at each iteration by a general-purpose nonlinear solver "fsolve" available in MATLAB®. "fmincon" takes about 20–25 iterations to converge depending on the operating voltage. For each iteration, "fsolve" takes about 20 iterations to converge. The details of modeling and optimization framework can be found in our previous publications [1,10].

3. Optimization studies

The base case design parameters are given in Table 3. The ranges of the decision variables considered in this study are provided in Table 4. The upper bound on the thickness of the ultrathin CL (t_{CL}) is kept at 5 μm so that the total thickness of all the CLs would not exceed 20 μm. Constraints are imposed on the volume fractions of voids, ionomer, and the solids in all the CLs to ensure that these fractions are non-negative and less than one.

3.1. Problem formulation-I

In formulation I, the cell current density is maximized for a given operating voltage. To understand the effects of platinum loading in each CL, the problem is solved with different upper bounds and constraints. Since the platinum loading in each CL in the base case design is 0.1 mg cm^{-2}, the upper bound on platinum loading for each CL is kept at 0.1 mg cm^{-2} in case 1. This ensures that the maximum overall platinum loading on the cathode side is 0.4 mg cm^{-2}. In the second case, the upper bound in each CL is kept at 0.25 mg cm^{-2}. The overall platinum loading is 1 mg cm^{-2} in this case. Cases 1 and 2 will be referred to as low Pt case and high Pt case, respectively, in our subsequent discussion.

Objective function: Maximization of i_{Cell} at a given V_{Cell}

$$\text{Decision variables}: f_{pt,i},\ f_{ionomer,i},\ m_{pt,i},\ t_{CL,i} \quad i = 1\text{–}4$$
$$\text{Subject to } 0 < \varepsilon_{r,i} < 1,\ 0 < \varepsilon_{ionomer,i} < 1,\ 0 < \varepsilon_{solid,i} < 1 \quad i = 1\text{–}4$$

The volume fractions of the voids, ionomer, and solids in the catalyst layer are a function of the optimization variables. For all the CLs (i = 1–4)

$$\varepsilon_{r,i} = 1 - \frac{m_{Pt,i}}{t_{CL,i} f_{Pt,i}} \left[\frac{1 - f_{Pt,i}}{\rho_C} + \frac{f_{Pt,i}}{\rho_{Pt}} + \frac{f_{ionomer,i}}{[1 - f_{ionomer,i}]\rho_{ionomer}} \right] \quad (1)$$

Table 5
Performance comparison between base case and optimized designs.

Voltage (V)	Current density (mA cm^{-2})		
	Base case design	Low Pt	High Pt
0.9	12.6	13.86	23.65
0.7	457.3	462.68	548.47
0.5	1223.71	1419.1	1481.76

$$\varepsilon_{ionomer,i} = \frac{1}{t_{CL,i}\rho_{ionomer}} \frac{m_{Pt,i}}{f_{Pt,i}} \left[\frac{f_{ionomer,i}}{1 - f_{ionomer,i}} \right] \quad (2)$$

$$\varepsilon_{solids,i} = 1 - \varepsilon_{r,i} - \varepsilon_{ionomer,i} \quad (3)$$

3.2. Discussion of the results

The comparison between the base case design and optimized conditions at various operating voltages for both the cases is shown in Table 5. In Table 5, it is observed that the performance enhancement is quite less at high operating voltages (low current densities) when the maximum platinum loading is the same as that of the base case design. On the other hand, the enhancement in the performance is almost double (12.6 mA cm^{-2} to 23.65 mA cm^{-2}) when the upper bound on the platinum loading is high (1 mg cm^{-2}) as seen in the first row of Table 5. This is due to considerable reduction of the activation losses by using high platinum content at low voltages. With an increase in the current density, two trends are observed. First, for the same low platinum loading (0.4 mg cm^{-2}), the optimized design improves the performance by roughly 16% (1223.71–1419.1 mA cm^{-2}). Second, the impact of higher platinum loading decreases as the operating voltage becomes lower mainly due to the increase in the ohmic and diffusion losses (high Pt case). The results also show that the optimum platinum loading hit the upper bound (0.4 mg cm^{-2}) in the low Pt loading case. In the high Pt case, though the optimum loading reached the upper bound at low current densities, it decreased at high current densities. These results indicate that the cell performance can be enhanced for the same platinum loading with the optimized design. However, since the best performance can be achieved at higher platinum loading and the objective of the first study is to maximize cell performance, detailed analysis presented below is performed with high Pt loading case only.

The comparison between the base case design and optimized conditions is shown in Fig. 2. Optimized cell current densities are shown as dashed lines as each current density is obtained using a

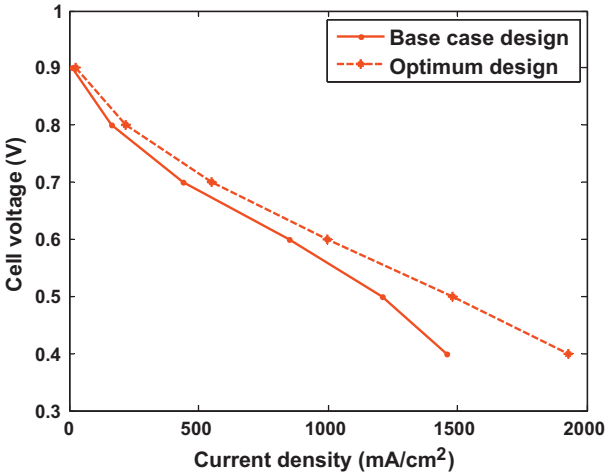

Fig. 2. Performance comparison between base case design and optimized conditions.

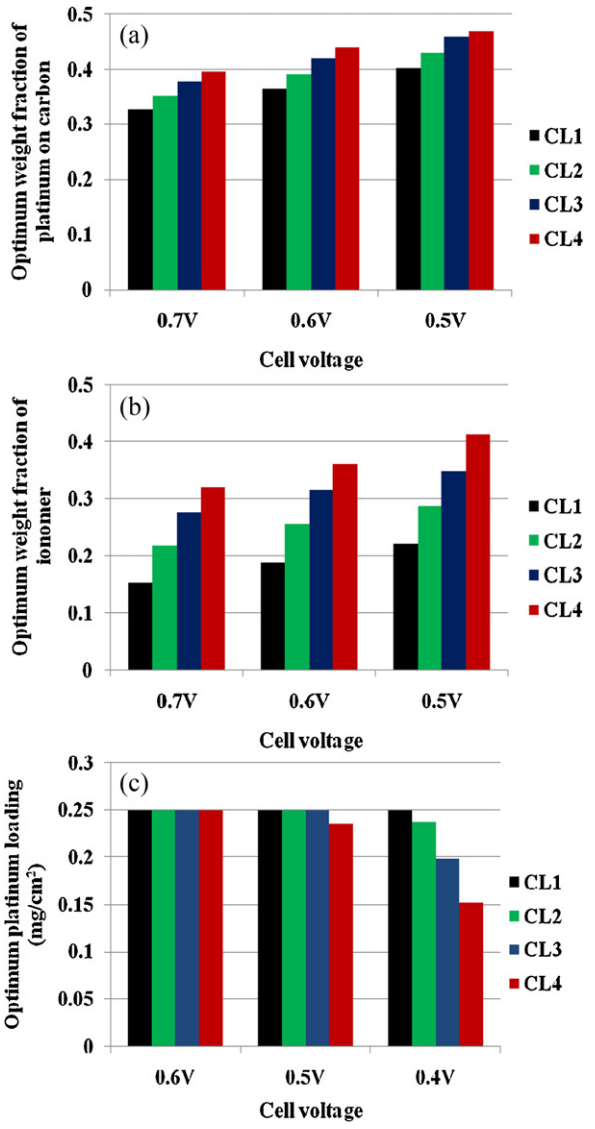

Fig. 3. Optimum distribution of (a) weight fraction of platinum on carbon, (b) weight fraction of ionomer and (c) platinum loading.

different set of catalyst layer parameters. Here, the base case design represents a single CL of thickness 20 μm. For the base case design performance curve, the design parameters are uniform in the entire catalyst layer. The optimum values of the CL parameters at various voltages are shown in Fig. 3. In these plots, CL1 corresponds to the MPL/CL interface and CL4 represents the CL/MEM interface.

Fig. 2 shows that there is significant improvement in the cell performance in all limiting regions. The improvement in the current density due to optimization is found to be about 33% at 0.4 V. At low current densities, the platinum loading in the optimal design hit the upper bound in all the CLs in order to minimize the activation losses. A similar trend is observed earlier in the studies with single CL [10].

As the ohmic and mass transport losses become significant at medium and high current densities, an increase in the ionomer and void fractions and reduction in the platinum loading are observed in all the CLs. The optimized design variables which support this observation can be seen from Fig. 3. An increase in the optimum weight fraction of ionomer can be observed in Fig. 3b with the increase in current density. Overall optimum platinum loading reduces by 16% when the operating voltage is reduced from 0.6 V to 0.4 V (Fig. 3c). The enhancement in the cell current density for

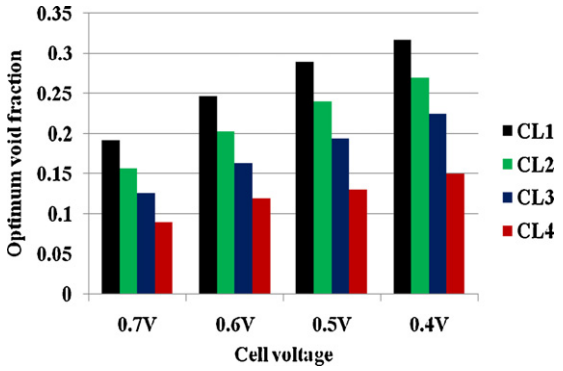

Fig. 4. Optimum distribution of void fractions in the CLs.

the optimal design is more significant at high current densities. This is due to a reduction in the cathode overpotential due to optimum distribution of voids and ionomer in all CLs. For example at a voltage of 0.5 V, the optimum void and ionomer fractions in CL1 through CL4 are 0.29, 0.24, 0.19, 0.13 and 0.27, 0.37, 0.45, 0.56, respectively. The optimum void and volume fractions of all the CLs at various operating voltages are shown in Figs. 4 and 5, respectively. As the flux of oxygen decreases from the MPL/CL interface towards the membrane due to the electrochemical reaction, the optimum void fractions also decrease. Since more amount of oxygen is required at higher current densities, a gradual rise in the optimum void fractions is observed from 0.7 V to 0.4 V in all the CLs.

The trend of the optimal ionomer fraction is opposite to that of the void fraction due to the consumption of protons from the CL/MEM interface towards the MPL/CL interface. The optimal distribution of the ionomer fraction is shown in Fig. 5. The thicknesses of the individual CLs are found to hit the upper bound of 5 μm in both high and low Pt loading cases. This study shows that the overall CL thickness of an optimized multiple CL PEMFC can be higher than the typical CL thickness of 10 μm or less used in the conventional single CL PEMFCs.

Although the optimum design values of the CLs are different for each operating voltage, an optimized MEA can be prepared only with one set of these parameters. To choose such a combination, the optimum design parameters corresponding to 0.5 V (power density is maximum at this voltage in the base case design) have been selected. The steady state simulations are carried out with this optimum design to find the power densities throughout the operating range. The comparison between the power–voltage curves of the base case design PEMFC and the PEMFC with optimally designed multiple CLs is shown in Fig. 6. The profile of oxygen partial pressure in the base case design and optimized designs is shown in

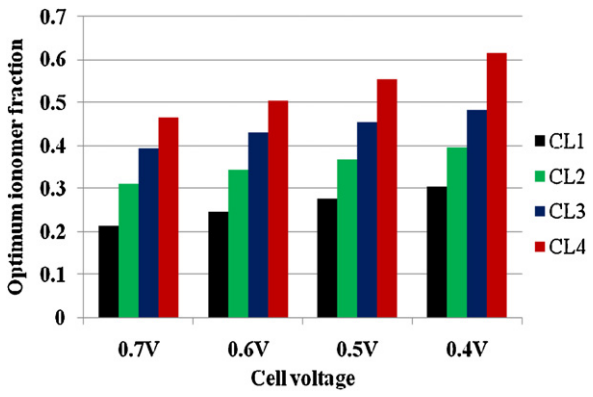

Fig. 5. Optimimum distribution of ionomer volume fractions in all CLs.

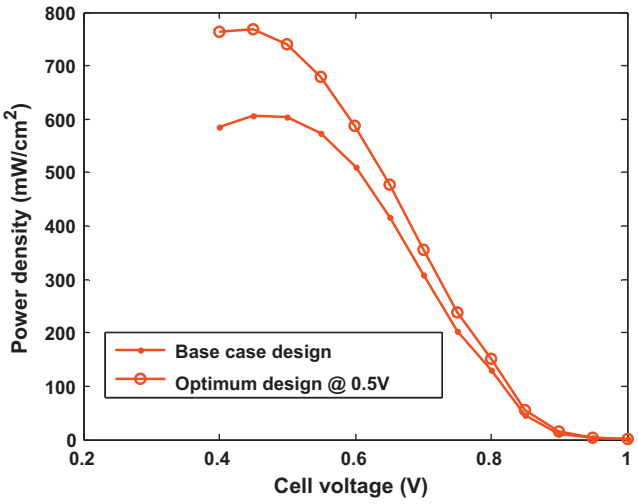

Fig. 6. Performance curves for the base case design and for the optimal design at 0.5 V.

Fig. 7. The partial pressure of oxygen is higher in most part of the CLs in the optimized multiple CL design. As explained above, this is due to the optimum distribution of voids in the multiple CL design.

3.3. Performance comparison between the optimized single CL cathode and multiple CL cathode

Fig. 8 shows a comparison between the performance of the optimized PEMFC with four CLs and the optimized PEMFC with single CL. In Fig. 8, the vertical axis represents the percentage increase in the cell performance compared to the base case design. The blue and red colors represent the performance of the optimally designed PEMFCs with single CL and multiple CLs, respectively. About 3–6% increase in the cell performance is observed with the PEMFC with optimally designed multiple CLs in comparison to the PEMFC with optimally designed single CL throughout the polarization range for the same platinum loading. Fig. 9 shows the difference between the power density achieved using optimized multiple CL PEMFC and optimized single CL PEMFC in the entire polarization range. As seen in the figure, the power density of the optimized multiple CL PEMFC is 23 mW/cm^2 higher at 0.5 V. For a large stack totaling thousands of cm^2 of area, the gain in total power generation can be very high.

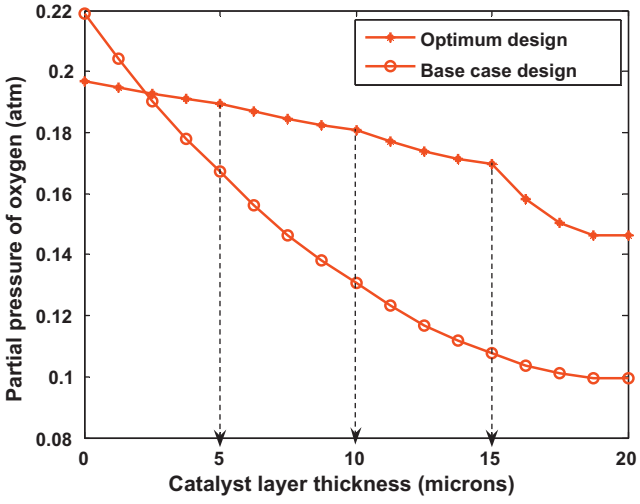

Fig. 7. Comparison of oxygen partial pressure between base and optimized designs.

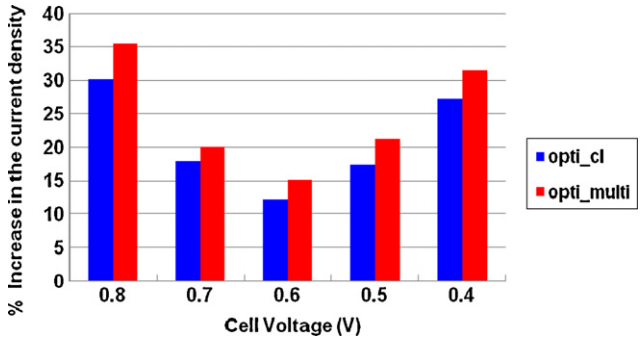

Fig. 8. Percent increase of current density of optimzed designs of single CL and multiple CLs over base case design.

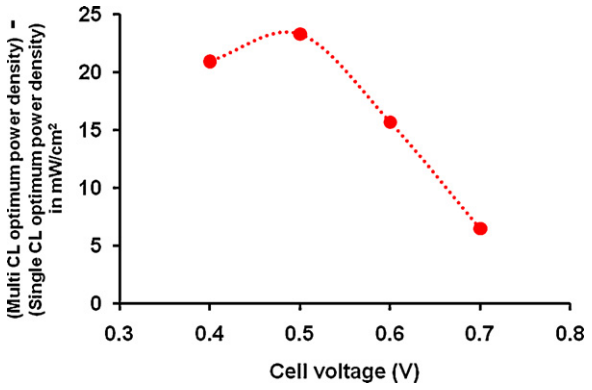

Fig. 9. Power density enhancement due to optimized multiple CL design over optimized single CL design.

3.4. Optimization formulation II

In this formulation, the platinum loading is minimized while maintaining the same performance as the base case design. In addition to the inequality constraints in formulation I, an additional constraint on the cell performance is considered ($i_{opt} = i_{base}$). Here, i_{opt} is the cell current density at the optimum design and i_{base} is the base case design current density.

Objective function: Maximization of i_{cell}/m_{Pt} at a given V_{Cell}

$$\text{Decision variables}: f_{pt,i},\ f_{ionomer,i},\ m_{pt,i},\ t_{CL,i} \quad i = 1\text{–}4$$

$$\text{Subject to } 0 < \varepsilon_{r,i} < 1,\ 0 < \varepsilon_{ionomer,i} < 1,\ 0 < \varepsilon_{solid,i} < 1 \quad i = 1\text{–}4,\quad i_{opt} = i_{base}$$

Optimization is performed at low and high currents, and the optimum platinum loadings are shown in Fig. 10. In Fig. 10, black and blue colors represent the platinum loading of the base case design and optimum designs with four CLs, respectively. There is a significant increase in the current generation per mg of catalyst

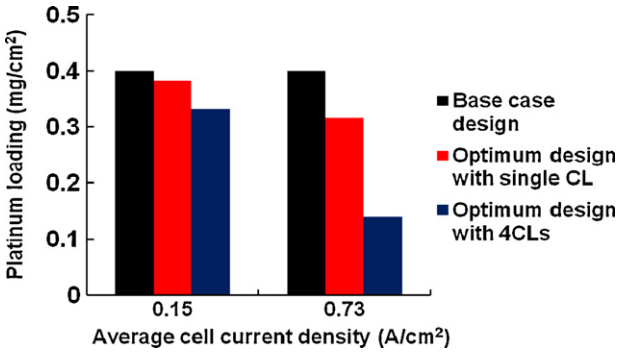

Fig. 10. Comparison of optimized and base case design platinum loadings.

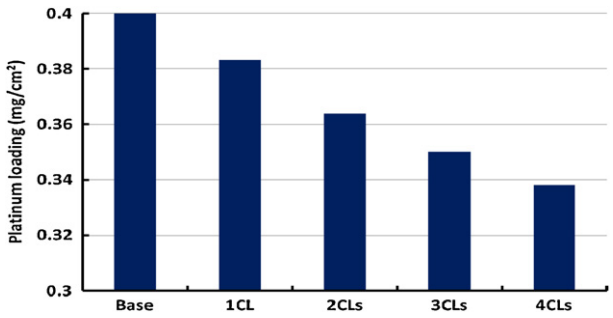

Fig. 11. Optimum platinum loading with single and multiple CLs cathode.

loading. In other words, there is a considerable reduction in the platinum loading for the same performance. When the current density is 0.15 A cm^{-2}, the optimum platinum loading is 0.33 mg cm^{-2} against the base case design platinum loading of 0.4 mg cm^{-2}. This is a 17% reduction in the platinum loading. When the current density increases further to 0.73 A cm^{-2}, the platinum reduction is about 60%. The platinum reduction is more at high current densities because of lower activation losses and stronger effect of ohmic and mass transport losses. Once again, the thicknesses of the individual CLs are found to hit the upper bound of 5 μm.

The obtained results are compared with the optimum design of a single CL. The red color in Fig. 10 represents the optimum platinum loading required to produce the same current density (0.15 A cm^{-2} and 0.73 A cm^{-2}) using the optimized single CL design.

Fig. 11 shows the optimized platinum loadings of single CL and multiple CL PEMFCs at 0.8 V in comparison to the base case design. The base case design conditions are given in Table 3. Here, optimization is carried out with the steady state model of a PEMFC cathode containing one, two, three, and four catalyst layers. The total thickness of the reaction medium is kept constant at 20 μm. The thickness of each CL is calculated such that the overall thickness is 20 μm. For example, while considering two CLs, the thickness of each CL is 10 μm. When a single CL (20 μm) is considered, a 4% reduction in platinum loading is achieved. With two CLs (each of 10 μm thickness), the reduction is 9%. The reductions in platinum loading with 3 and 4 CLs are 12.5% and 15.5%, respectively. As the number of catalyst layers increases, the design variables also increase. As a result, flexibility in selecting the optimum design variables also increases.

4. Conclusions

In this paper, two optimization studies of a PEMFC with an innovative multiple CL cathode using a two-dimensional two-phase model are presented. The decision variables used in these studies are the design parameters of all CLs. In the first optimization study, the cell performance is maximized. The optimization improves the cell current density by about 15% in the high current density region and by about 85% in the low current density region. The PEMFC with optimized multiple CLs shows an improvement of 3–6% in the cell performance over the optimized PEMFC with single CL. In the second optimization study, the platinum loading has been minimized for a given performance. The optimization results in a reduction of 17–60% platinum loading at various current densities in comparison to the base case design without sacrificing the performance. When the optimization is performed with single, two, three, and four catalyst layers at 0.8 V, it is observed that a higher reduction in the platinum loading can be achieved with an increase in the number of CLs. This study shows that an optimized multiple layered PEMFC is a promising option to improve the performance of the PEMFCs and to decrease its cost.

References

[1] M. Srinivasarao, D. Bhattacharyya, R. Rengaswamy, S. Narasimhan, Int. J. Hydrogen Energy 35 (2010) 6356.
[2] A.D. Taylor, E.Y. Kim, V.P. Humes, J. Kizuka, L.T. Thompson, J. Power Sources 171 (2007) 101.
[3] K.-H. Kim, H.-J. Kim, K.-Y. Lee, J.H. Jang, S.-Y. Lee, E. Cho, I.-H. Oh, T.-H. Lim, Int. J. Hydrogen Energy 33 (2008) 2783.
[4] H.-N. Su, Q. Zeng, S.-J. Liao, Y.-N. Wu, Int. J. Hydrogen Energy 35 (2010) 10430.
[5] R. Madhusudana Rao, D. Bhattacharyya, R. Rengaswamy, S.R. Choudhury, J. Power Sources 173 (2007) 375.
[6] D. Song, Q. Wang, Z. Liu, M. Eikerling, Z. Xie, T. Navessin, S. Holdcroft, Electrochim. Acta 50 (2005) 3347.
[7] H.H. Lin, C.H. Cheng, C.Y. Soong, F. Chen, W.M. Yan, J. Power Sources 162 (2006) 246.
[8] M. Secanell, B. Carnes, A. Suleman, N. Djilali, Electrochim. Acta 52 (2007) 6318.
[9] P. Jain, L.T. Biegler, M.S. Jhon, Electrochem. Solid-State Lett. 11 (2008) B193.
[10] M. Srinivasarao, D. Bhattacharyya, R. Rengaswamy, S. Narasimhan, Chem. Eng. Res. Des. 89 (2011) 10.